# Calibrating a machine spindle on the nanoscale: a new error separation technique

S. Cappa, D. Reynaerts, F. Al-Bender
*KU Leuven Department of Mechanical Engineering, Belgium*

## Abstract

In this work, a nanometre accurate spindle error motion separation technique is proposed and validated. This new measurement method is the result of an elaborate error analysis of the Donaldson reversal, Grejda reversal and the multiprobe technique. The principle is in fact an improvement of the multiprobe technique. The measurement angles of the multiprobe technique are optimized, as this method suffers from suppressed harmonic components. Experimental tests show the sub-nanometre measurement uncertainty and repeatability as well as the effectiveness of the proposed spindle error motion separation technique. The influence of the measurement angles on the measured radial error motion and artifact form error is examined.

## 1 Introduction

Today, workpiece tolerances are becoming more stringent. Nanometre-level tolerances are no longer an exception. This stress the need for ultra-precision machine spindles as they considerable contributes to the overall accuracy of a precision machine [1]. However, in order to quantify the error motion of a spindle on the nanoscale, accurate spindle error motion separation techniques are required. Over the years, many error separation techniques have been described in the literature. However, most of them are still prone to measurement errors and uncertainties because of a poor hardware design and careless implementation of the separation technique. This work aims at the design of a novel spindle error motion separation technique reducing the measurement uncertainty to the sub-nanometre level. To this end, the measurement uncertainty of the Donaldson reversal [2], Grejda reversal [3] and the multiprobe technique [4] are compared based on an elaborated error analysis using real data of the radial and axial error motion of a nanometre accurate aerostatic rotary table and the out-of-roundness of a lapped spherical artifact.

Based on these results, a new spindle error motion separation technique is proposed and validated.

## 2 Background

The rotor of a spindle has ideally one degree of freedom, i.e. rotation about the z-axis (by convention). Any motion in the remaining five degrees of freedom is referred to as error motion and is described in the ANSI/ASME B89.3.4M standard. The error motion of a spindle is indicated by the radial error motion (translation perpendicular to the axes of rotation, i.e. x- and y-direction at a specified height), the axial error motion (translation coaxial to the axes of rotation, i.e. z-direction) and the tilt error motion (rotation around the x- and y-axis). The error motion of an ultra-precision aerostatic spindle is usually characterized with the use of a lapped spherical artifact (master ball) which is mounted on top of the rotor. A spindle measurement includes the effect of both the error motion of the spindle and the out-of-roundness (form error) of the artifact. However, the out-of-roundness of such an artifact may equal or even exceed the spindle error motion, i.e. between 10 and 30 nm. As a result, the artifact out-of-roundness necessitates the use of a spindle error motion separation technique to extract the error motion and artifact form error from the raw measurement data; no method relies upon a calibrated artifact.

## 3 Error budget

The overall error and measurement uncertainty of the Donaldson reversal, Grejda reversal and multiprobe technique are compared in this section based on an error analysis. The measurement uncertainty is mainly determined by the specific operations required by each method, as imperfectly repositioned sensor(s) and artifact, as well as varying sensor sensitivities, have an adverse effect on the accuracy.

The typical errors introduced while separating the error are observed and an expression is derived in order to calculate the overall error and measurement uncertainty of each method based on an error budget and Monte-Carlo simulation, respectively[1]. Table 1 lists all the error components per separation technique, as well as the maximal and resulting measurement errors $\varepsilon(\theta)$. The maximal error defines the domain of possible errors per error component. The measurement errors $\varepsilon(\theta)$, on the other hand, are all calculated assuming a maximal error, identifying the error components that impede sub-nanometre accuracy and repeatability. The overall error in Tab. 1 of each method is calculated by a combinatorial rule, originally suggested by Hocken [5], that predicts an overall system error value based on the means of the arithmetic sum and RMS of the individual error values. The arithmetic sum of the error

[1] The description and derivation of the errors falls outside the scope of this paper.

components are unreasonably high and represents and upper bound. This approach is therefore extremely conservative as the probability of all errors reaching maxima at the same time is very unlikely. The RMS sum, on the other hand, represents a lower bound of the overall error. The predicted error would be overly optimistic in this case, since many of the errors cannot be assumed to be uncorrelated and some are dependent on common sources. Hocken's rule has proven to be remarkably robust and is well accepted in the field of precision engineering. The measurement uncertainty, on the other hand, of each error separation technique is determined by a Monte-Carlo simulation, performing 300.000 calculations of $\varepsilon(\theta)$ for each error component, assuming a uniform probability distribution for the error domain. For this purpose, real data of the radial and axial error motion of an aerostatic rotary table and the form error of a spherical artifact is used.

Table 1: Maximal errors and corresponding measurement errors per error component for each error motion separation techniques under study.

| | **Error component** | **Donaldson** | | **Grejda** | | **Multiprobe** | |
|---|---|---|---|---|---|---|---|
| | | max. error | $\epsilon(\theta)$ [nm] | max. error | $\epsilon(\theta)$ [nm] | max. error | $\epsilon(\theta)$ [nm] |
| **ARTIFACT** | positioning error [°] | 0.3 | 0.3 | 0.1 | 0.1 | n/a | n/a |
| | eccentricity [$\mu$m] | 20 | 7.9 | 5 | 0.5 | 0.5 | 0.005 |
| **SENSOR** | positioning error [°] | 0.2 | 0.2 | n/a | n/a | 0.2 | 0.1 |
| | tilt error [°] | 0.5 | 0.05 | n/a | n/a | 0.5 | 0.05 |
| | misalignment [°] | 0.2 | $\approx 0$ | 0.2 | $\approx 0$ | 0.2 | 0.02 |
| **INDEX. TABLE** | positioning error [°] | n/a | n/a | 0.02 | 0.1 | n/a | n/a |
| **ERROR [nm]** | | 6.2 | | 0.5 | | **0.12** | |
| **UNCERTAINTY [nm]** | | 2.35 | | 0.15 | | **0.04** | |

### 3.1 Conclusion

As can be seen from Tab. 1, the multiprobe technique has the lowest overall error and measurement uncertainty, i.e. 0.12 nm and 0.04 nm, respectively. The Donaldson reversal technique, on the other hand, has the highest overall error and measurement uncertainty. This can be attributed, as indicated in Tab.1, to the fact that the artifact must be indexed by 180° between two measurements, which can lead to a large eccentricity and, consequently, to a first and second order error as shown by Grejda in [3]. This is partially improved by Grejda by the use of a special designed reversal chuck with a lapped spherical pilot.

## 4 Principle

The major advantage of the multiprobe technique, with respect to the reversal techniques, is the fact that the artifact is never moved. Nevertheless, the main drawback of this method is that the sensor must be indexed precisely over an angle $\alpha$ and $\beta$ if one sensor is used (see Fig. 2). However, this can be overcome by combining the advantages of the multiprobe and Grejda reversal technique.

Instead of indexing the sensor, the error motion is measured consecutively under three different orientations by rotating the stator using a high-precision indexation table, like Grejda improved the Donaldson reversal technique. This is more accurate and much easier to implement. As a result, only a single sensor and artifact is used, which are never moved during the analysis. This bypasses accurate indexing of the artifact and sensor(s) during testing, as well as the effects of varying sensor sensitivities if multiple sensors are used. The principle is shown in Fig. 1. The error components of this new error separation technique, with its maximal and resulting measurement errors $\varepsilon(\theta)$, are listed in Tab. 2. The overall error and measurement uncertainty of the proposed method is of sub-nanometre level namely 0.024 nm and 0.01 nm, respectively. The results, as shown in Tab. 2, indicate that the accuracy of the improved multiprobe technique is remarkably higher than the conventional multiprobe technique. These theoretical results will be validated experimentally in section 6 by measuring the radial error motion of a nanometre level aerostatic rotary table designed and produced in our lab.

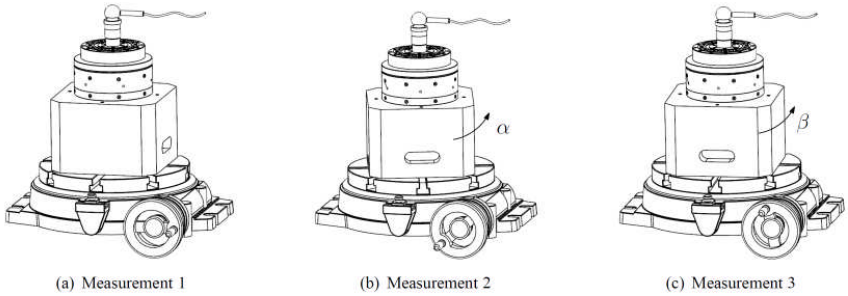


Figure 1: Principle of the new spindle error motion separation technique based on the modified multiprobe technique rotating the stator three consecutive times using a high-precision indexation table.

## 5 Optimisation of the measurement angles

As Whitehouse [4] observed, the conventional multiprobe technique is not a true reversal technique. Depending on the number of probes and their locations, the multiprobe technique is insensitive to some harmonic components $k$ of the spindle error motion. Therefore, the error motion cannot be reconstructed accurately on nanometer level if these harmonics are present. This problem of suppressed harmonics is due to the complex harmonic weighting function W(k), which can be seen as the transfer function of the measurement data to the

Table 2: Maximal errors and corresponding measurement errors per error component of the error separation technique proposed in this work.

| | Error component | Cappa | |
|---|---|---|---|
| | | max. error | $\epsilon(\theta)$ [nm] |
| **ARTIFACT** | positioning error [°] | n/a | n/a |
| | eccentricity [$\mu$m] | 0.5 | 0.005 |
| **SENSOR** | positioning error [°] | n/a | n/a |
| | tilt error [°] | n/a | n/a |
| | misalignment [°] | 0.2 | 0.02 |
| **INDEX. TABLE** | positioning error [°] | 0.02 | 0.01 |
| **ERROR [nm]** | | **0.024** | |
| **UNCERTAINTY [nm]** | | **0.01** | |

artifact form error, approaches zero at certain harmonics for several combinations of the measurement angles α and β, which are indicated in Fig. 2. However, the problem of suppressed harmonics can be overcome by an optimization of the measurement angles α and β, namely by maximizing the minimal absolute value of the complex harmonic weighting function W(k). Marsh already determined in [6] a suitable value for α and β as 99° 50' and 202° 30', respectively. However, he did not described how he got these values in his report. Therefore, in this work, we formulate the general optimisation problem in order to determine most appropriate values for α and β.

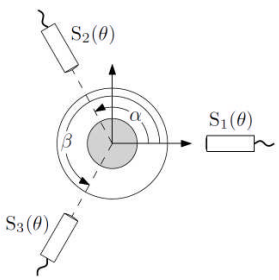


Figure 2: Schematic representation of the conventional multiprobe technique indicating the measurement angles α and β.

The optimisation problem can be formulated as follows:

Maximize: min |W(k)| k = 2,...,N
Subject to: 20° < α < 320° \ {180°}
40° < β < 340° \ {180°}
β - α ∉ ]179°, 181°[

Wherein the complex harmonic weighting function W(k) is expressed as:

$$W(k) = 1 + a\, e^{-jk\alpha} + b\, e^{-jk\beta}$$

and the coefficients a and b as:

$$a = -\sin\beta / (\sin(\beta - \alpha)) , \quad b = \sin\alpha / (\sin(\beta - \alpha))$$

As this optimization problem is two dimensional and comprises various local maxima, i.e. not a convex optimization problem, the minimal value of |W(k)| is determined for all possible combinations of $\alpha$ and $\beta$ between the $2^{nd}$ and $150^{th}$ harmonic. This is shown in Fig. 3. Black colored regions depict combinations of $\alpha$ and $\beta$ where certain harmonics will be suppressed during separation, i.e. min |W(k)| near zero. These combinations must therefore be avoided. White colored regions, on the other hand, represent a high value of min |W(k)| and are thus preferred. From Fig. 3 it is apparent that the set defined by the minimum value of |W(k)| has some self-similar patterns, i.e. fractals. The consequence of this self-similar pattern is that no optimum for $\alpha$ and $\beta$ can be found. However, one of the optimal combinations is $\alpha = 100° 24′$ and $\beta = 231° 2′$, as indicated in Fig. 3. These angles are chosen because they line up with the marks on the indexation table. Moreover, Fig. 3 indicates that the well-known example of $\alpha = 120°$ and $\beta = 240°$ will result in an incorrect separation (black colored region), while the measurement angles proposed by Marsh are located in a 'danger zone'. This is validated experimentally further in this work.

## 6 Experimental validation

Before discussing the various experiments and results, the test setup shown in Fig. 4 is described. The spindle under test, an aerostatic rotary table developed in [7], is partially mounted in a granite block which is placed on a high-precision indexation table. The capacitive probe, placed on a *xyz*-stage, targets on the centre of a 1"∅ lapped spherical artifact which, in turn, is screwed on the top plate of the aerostatic rotary table. This top plate is mounted on the rotor. The whole setup is placed on a granite surface plate which is on an air damped table to reduce the influence of external vibrations. Finally, the *xyz*-stage, with its capacitive probe, is screwed on a granite stand which also is placed on the surface plate.

In the next experiments, the proposed error motion separation technique will be validated. Firstly the measurement uncertainty is determined. Secondly, the effectiveness of the separation method is proofed. Lastly, the influence of the measurement angles $\alpha$ and $\beta$ is examined.

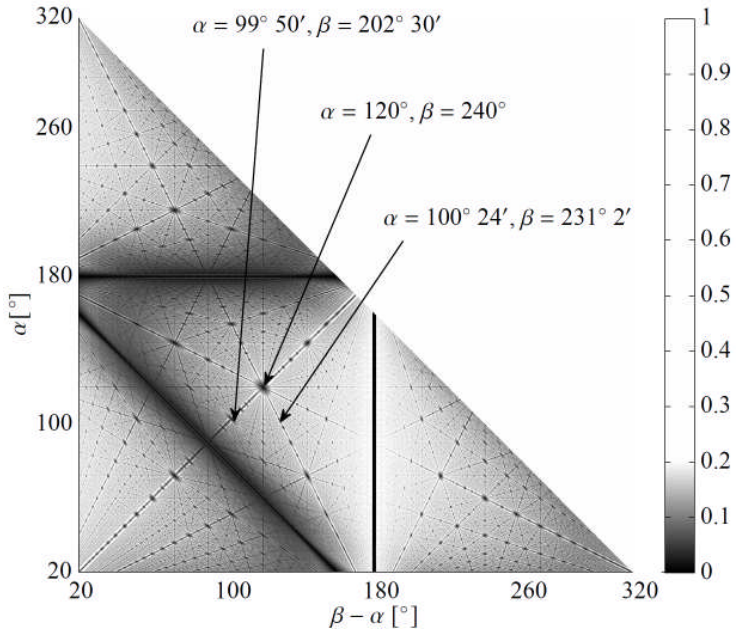


Figure 3: Minimal value of |W(k)| for each combination of α and β. Black colored regions depicts a low value of min |W(k)|, i.e. harmonic suppression, while, on the other hand, white colored regions are preferred. One of the optimal combinations of α and β is 100° 24′ and 231° 2′, respectively.

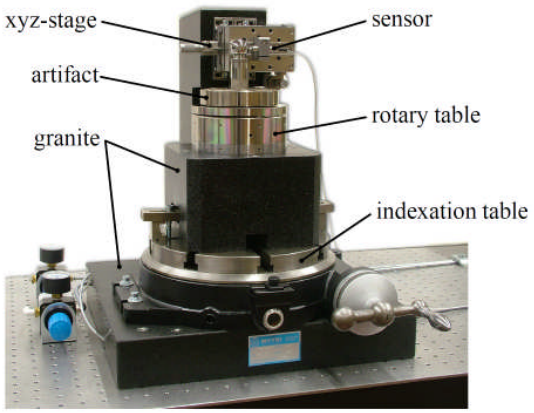


Figure 4: Test setup of the proposed spindle error motion separation technique.

### 6.1 Measurement uncertainty

The measurement uncertainty of the error separation technique proposed in this work is examined first. This is determined by measuring the radial error motion

of the aerostatic rotary table and the artifact form error ten times. Table 3 represents the results obtained from the test. As can be seen from the table, both the radial error motion and artifact form error has a measurement uncertainty of sub-nanometre level. Contrary to expectations, the measurement uncertainty is higher than the theoretical determined uncertainty in section 4, i.e. 0.455 nm and 0.727 nm instead of 0.01 nm. A possible explanation for this might be that the theoretical error analysis was limited to the errors directly related to the specific operations required by each error separation technique. Several others, like DAQ and instrument errors, noise, vibrations and temperature fluctuations were, however, not taken into account in this analysis.

Table 3: The radial error motion and artifact form error measured ten times determining the sub-nanometer level measurement uncertainty of the proposed error separation technique.

| | **Radial error motion** [nm] | **Artifact form error** [nm] |
|---|---|---|
| 1 | 9.1 | 32.1 |
| 2 | 9.7 | 33.1 |
| 3 | 10.3 | 32.9 |
| 4 | 9.5 | 34.2 |
| 5 | 9.8 | 33.8 |
| 6 | 9.7 | 33.5 |
| 7 | 9.6 | 33.4 |
| 8 | 9.3 | 34.7 |
| 9 | 8.6 | 33.5 |
| 10 | 9.7 | 34.0 |
| $\sigma$ | **0.455** | **0.727** |

## 6.2 Effectiveness of the separation technique

Although, the measurement uncertainty is of sub-nanometer level, this does not guarantee a correct separation of the errors. This, however, can be examined experimentally by applying an artificial error to the lapped spherical artifact while performing a separation. This error must be completely reproduced in the form error of the artifact after separation, while the radial error motion should not be affected. To this end, an ink mark was applied on the artifact. The separated radial error motion and artifact form error measured with and without ink mark are, in turn, compared in Fig. 5. From this figure we can see that the radial error motion is the same for the two measurements, apart from a few minor differences. The ink mark, on the other hand, is reproduced completely in the polar plot of the artifact form error in Fig. 5.

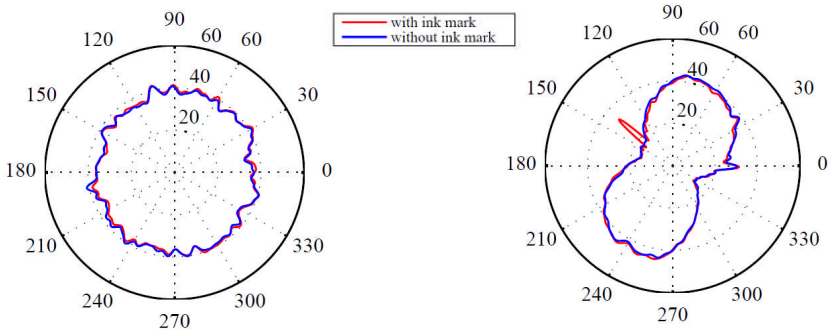


(a) Radial error motion (b) Artifact form error

Figure 5: Comparison of the radial error motion and artifact form error measured with and without ink mark in order to validate the effectiveness of the proposed error separation method.

### 6.3 Influence of the measurement angles α and β

In this experiment, the influence of the measurement angles α and β is analysed on the measured radial error motion and artifact form error using the proposed separation technique. This is done for α and β equal to 100° 24’ and 231° 2’ (optimal angles), 99° 50’ and 202° 30’ (Marsh) and the extreme case of 120° and 240°, respectively. The polar plots in Fig. 6 show a comparison between the measurement results for these different values of α and β. The radial error motion and artifact form error of the optimal measurement angles, proposed in section 4, and the measurement angles used by Marsh are the same within 2 nm. However, it is clear from this figure that both results are not identical. This difference may be explained by the fact that the measurement angles proposed by Marsh lie in a darker (less optimal) zone compared with our optimal measurement angles, as already indicated in Fig. 3. Further, the results in Fig. 6 for α = 120° and β = 240° show a significant difference. This can be attributed to the phenomenon of harmonic suppression, as is apparent from Fig. 3.

## 7 Conclusion

A novel spindle error motion separation technique with sub-nanometre measurement uncertainty is proposed and validated in this work, based on an elaborate error analysis of three commonly used spindle error motion separation techniques. The novel spindle error motion separation technique is based on the conventional multiprobe technique. However, instead of indexing one sensor or using multiple sensors with a different sensitivity, the error motion is measured consecutively under three different orientations by rotating the stator with the use of a high-precision indexation table.

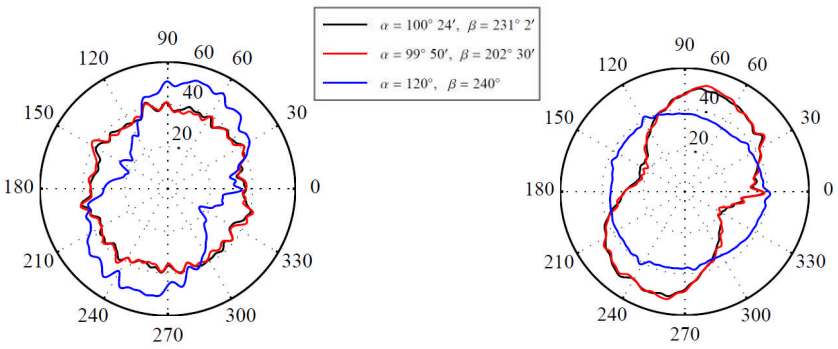


(a) Radial error motion (b) Artifact form error

Figure 6: Influence of the measurement angles α and β on the measured radial error motion and artifact form error.

Repeatability tests on the radial error motion of an aerostatic rotary table shows sub-nanometre level measurement uncertainty of the proposed error separation technique as well as the effectiveness of the method. Further, the measurement angles are optimized discarding the problem of harmonic suppression: α = 100° 24' and β = 231° 2' as poorly chosen measurement angles result in large measurement errors.

## 8 Acknowledgement

This research is sponsored by the Fund for Scientific Research - Flanders (F.W.O.) under Grant G037912N. The scientific responsibility is assumed by its authors. The authors acknowledge the support of Professional Instruments in providing them with a lapped spherical artifact.

## References

[1] J. Bryan, R. Clouser, E. Holland, Spindle accuracy, American Machinist 111(25) (1967) 149-164.
[2] R. R. Donaldson, A simple method for separating the spindle error from test ball roundness error, CIRP Annals 21(1) (1972) 125–126.
[3] R. D. Grejda, Use and calibration of ultraprecision axes of rotation with nanometer level metrology, Ph.D. thesis, Penn State University (2002).
[4] D. J. Whitehouse, Some theoretical aspects of error separation techniques in surface metrology, J. Phys. E. 9 (1976) 531–536.
[5] D. C. Thompson, B. Fix, Comparison between predicted and actual accuracies for an ultra-precision cnc measuring machine (1995).
[6] E. R. Marsh, D. Arneson, D. Martin, A comparison of reversal and multiprobe error separation, Precision Engineering 34 (2010) 85–91.
[7] Cappa et. al. Reducing the error motion of an aerostatic journal bearing. Proc. of the 12th euspen Int. Conf.: Vol. 1. Stockholm,Sweden, 435-438.